NASA TECHNICAL NOTE

NASA TN D-5622

NASA TN D-5622

THE EFFECTS OF A NONRIGIDLY SUPPORTED BALLAST ON THE DYNAMICS OF A SLENDER BODY DESCENDING THROUGH THE ATMOSPHERE

by Gerald N. Malcolm

Ames Research Center
Moffett Field, Calif.

NATIONAL AERONAUTICS AND SPACE ADMINISTRATION • WASHINGTON, D. C. • JANUARY 1970

1. Report No. NASA TN D-5622	2. Government Accession No.	3. Recipient's Catalog No.
4. Title and Subtitle THE EFFECTS OF A NONRIGIDLY SUPPORTED BALLAST ON THE DYNAMICS OF A SLENDER BODY DESCENDING THROUGH THE ATMOSPHERE		5. Report Date January 1970 6. Performing Organization Code
7. Author(s) Gerald N. Malcolm		8. Performing Organization Report No. A-3291
9. Performing Organization Name and Address NASA Ames Research Center Moffett Field, Calif., 94035		10. Work Unit No. 124-07-02-14-00-21 11. Contract or Grant No.
12. Sponsoring Agency Name and Address NATIONAL AERONAUTICS AND SPACE ADMINISTRATION Washington, D. C., 20546		13. Type of Report and Period Covered TECHNICAL NOTE 14. Sponsoring Agency Code

15. Supplementary Notes

16. Abstract

The effects of a nonrigidly supported ballast on the dynamic behavior of a slender body with linear aerodynamics descending through the atmosphere in planar motion are investigated. The equations of motion of both the main vehicle and the spring-mounted ballast are derived and specific examples are presented to illustrate the resulting motions. Divergent oscillations of the main vehicle occurred for those conditions near the coalescence of frequency of the main body and ballast motions. Divergence occurred earlier in the flight when spring stiffness was decreased, or when ballast damping was increased for a given spring stiffness.

17. Key Words Suggested by Author: Dynamics of slender entry body with nonrigid ballast	18. Distribution Statement: Unclassified - Unlimited		
19. Security Classif. (of this report): Unclassified	20. Security Classif. (of this page): Unclassified	21. No. of Pages: 20	22. Price*: $3.00

*For sale by the Clearinghouse for Federal Scientific and Technical Information Springfield, Virginia 22151

SYMBOLS

A	reference area, $\frac{\pi d^2}{4}$, ft^2
b	damping coefficient for ballast system, slugs/sec
C_m	pitching-moment coefficient, $\frac{\text{pitching moment}}{q_\infty Ad}$
C_{m_α}	pitching-moment curve slope of cone alone (without ballast), $\frac{\partial C_m}{\partial \alpha}$
$C_{m_{\alpha_{sys}}}$	pitching-moment curve slope of system (cone plus ballast)
CMQ	damping-in-pitch parameter $C_{m_q} + C_{m_{\dot{\alpha}}} - \frac{C_{N_\alpha}}{m_1 d^2 / I_{sys}}$
$C_{m_q} + C_{m_{\dot{\alpha}}}$	damping-in-pitch derivative, $\frac{\partial C_m}{\partial (qd/V)} + \frac{\partial C_m}{\partial (\dot{\alpha} d/V)}$
C_{N_α}	normal-force curve slope
C_x	axial-force coefficient
d	reference length (diameter of cone base), ft
f_{o_y}	natural frequency of ballast attached to platform of infinite mass, $f_{o_y} = \frac{1}{2\pi}\sqrt{\frac{k}{m_2}}$, cps
f_{o_α}	natural frequency of cone with rigidly mounted ballast, $f_{o_\alpha} = \frac{1}{2\pi}\sqrt{\frac{q_\infty Ad C_{m_{\alpha_{sys}}}}{I_{sys}}}$, cps
f_y	natural frequency of ballast when attached to moving cone, cps
f_α	natural frequency of cone with nonrigidly mounted ballast, cps
h	altitude, ft
I	sum of moments of inertia of ballast and cone about transverse axes through their centers of gravity, $slug\text{-}ft^2$
I_{sys}	moment of inertia about a transverse axis through the center of gravity of the cone-ballast system, $slug\text{-}ft^2$, $I + \frac{m_1 m_2}{m_1 + m_2} x_b^2$

k	spring constant, lb/ft
M_o	total pitching moment of cone alone
m_1	mass of cone alone, slugs
m_2	mass of ballast, slugs
q	pitching velocity, rad/sec
q_∞	free-stream dynamic pressure, lb/ft^2
t	flight time, sec
V	velocity along flight path, ft/sec
x	horizontal displacement from inertial reference, ft
x_b	distance from cone center of gravity ($x_{cg_{cone}}$) to ballast, ft
$x_{cg_{cone}}$	center-of-gravity location of cone alone, ft
$x_{cg_{sys}}$	center-of-gravity location of cone-ballast system, ft
x_{cp}	center-of-pressure location on cone, ft
y	displacement of ballast normal to cone axis of symmetry, ft
z	vertical displacement from inertial reference, ft
α	angle of attack, rad
γ	swerve angle, rad
η_R	ratio of damping to critical damping for ballast system, $\frac{b}{2\sqrt{km_2}}$
θ	pitch angle, rad
ρ	atmospheric density, $slugs/ft^3$
ω_1	natural frequency of cone in equation (13), $2\pi f_\alpha$, rad/sec
ω_2	natural frequency of ballast in equation (13), $2\pi f_y$, rad/sec
$\dot{(\ )}$	first derivative with respect to time, $\frac{d}{dt}$

$(\ddot{})$	second derivative with respect to time, $\frac{d^2}{dt^2}$
$(\ )_{fc}$	frequency coalescence

THE EFFECTS OF A NONRIGIDLY SUPPORTED BALLAST ON THE DYNAMICS OF A SLENDER BODY DESCENDING THROUGH THE ATMOSPHERE

By Gerald N. Malcolm

Ames Research Center

SUMMARY

The effects of a nonrigidly supported ballast on the dynamic behavior of a slender body with linear aerodynamics descending through the atmosphere in planar motion are investigated. The equations of motion of both the main vehicle and the spring-mounted ballast are derived and specific examples are presented to illustrate the resulting motions. Divergent oscillations of the main vehicle occurred for those conditions near the coalescence of frequency of the main body and ballast motions. Divergence occurred earlier in the flight when spring stiffness was decreased, or when ballast damping was increased for a given spring stiffness.

INTRODUCTION

Many atmosphere-entry bodies, particularly slender bodies, are ballasted for adequate aerodynamic static stability. The ballast typically is heavy, dense, and difficult to support in a perfectly rigid fashion under dynamic conditions. The purpose of this paper is to report some effects on the vehicle dynamics when the ballast is not rigidly supported but oscillates as part of a coupled system with the main vehicle.

The differential equations of planar motion for a body with linear aerodynamics and a flexibly mounted mass are derived; and a specific example - a slender cone with spring-mass system to represent the ballast arrangement - is used to illustrate some of the possible results of vehicle-ballast dynamic interaction.

EQUATIONS OF MOTION

The system to be analyzed consists of a main body - in this case, a slender cone - and an internal nonrigidly supported ballast simulated by a simple spring-mass system. The cone motion is restricted to one degree of freedom in rotation and two degrees of freedom in translation, all in a single plane. The ballast motion is restricted to this same plane and has one-dimensional motion perpendicular to the cone axis. The system is shown in

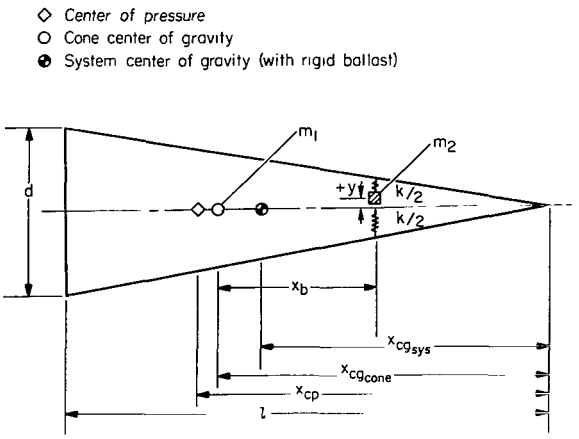

Sketch (a)

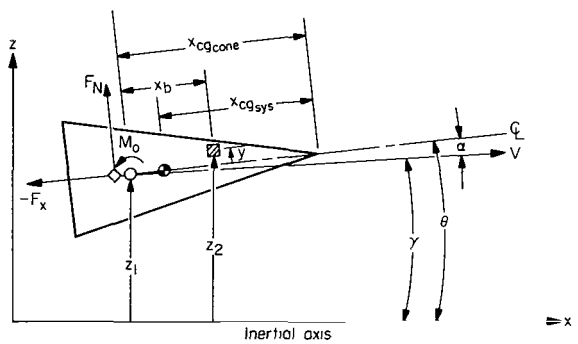

Sketch (b)

sketch (a) where m_1 and m_2 are the masses of the cone and ballast, respectively. The centers of gravity of the cone alone, $x_{cg_{cone}}$, and of the system, $x_{cg_{sys}}$, (if the ballast were rigidly mounted) are shown with the aerodynamic center of pressure, x_{cp}. The distance of the ballast center of gravity from the reference point (i.e., the center-of-gravity position of the cone alone) is x_b. Note that $x_{cg_{sys}}$, the center of gravity of a system consisting of a vehicle with moving parts, does not remain stationary so is not a suitable reference. The total spring constant in the ballast system is k.

This system is shown again in sketch (b) with an inertial reference system and body-fixed aerodynamic forces F_x and F_N. The center of rotation for the aerodynamic moment, M_o, is the center of gravity of the cone alone. Shown also are angles θ, the angular position of the cone with respect to the inertial x-axis, α, the angle of attack, and γ, the swerve angle.

Referring to sketch (b) we can write the differential equations of motion. If small angles are assumed, for example,

$$\sin(\alpha) \cong \alpha$$

$$\cos(\alpha) \cong 1$$

and gravity forces are neglected, the moment and force relationships are

$$I\ddot{\theta} = M_o + (ky + b\dot{y})x_b + m_2\ddot{x}y \quad (1)$$

$$m_1\ddot{z}_1 = F_N + ky + b\dot{y} \quad (2)$$

$$m_2 z_2 = ky - b\dot{y} \quad (3)$$

$$\ddot{z}_2 = \ddot{z}_1 + x_b\ddot{\theta} + \ddot{y} \quad (4)$$

where

$$M_o = C_{m_\alpha} \alpha q_\infty Ad + C_{m_q} q_\infty Ad \left(\frac{d}{V}\right) \dot{\theta} + C_{m_{\dot{\alpha}}} q_\infty Ad \left(\frac{d}{V}\right) \dot{\alpha}$$

$$F_N = C_{N_\alpha} \alpha q_\infty A$$

$$F_x = C_x q_\infty A$$

$$\ddot{x} = - \frac{F_x}{m_1 + m_2}$$

Note that the aerodynamic normal force, F_N, and the restoring moment, M_o, were assumed to vary linearly with angle of attack and that the axial force, F_x, was assumed constant. From sketch (b)

$$\theta = \alpha + \gamma \tag{5}$$

$$\dot{\theta} = \dot{\alpha} + \dot{\gamma} \tag{6}$$

$$\ddot{\theta} = \ddot{\alpha} + \ddot{\gamma} \tag{7}$$

$$\dot{x} = V \tag{8}$$

$$\ddot{x} = \dot{V} = - \frac{C_x q_\infty A}{m_1 + m_2} \tag{9}$$

$$\dot{z}_1 = V\gamma \tag{10}$$

$$\ddot{z}_1 = V\dot{\gamma} + \dot{V}\gamma \tag{11}$$

From equation (11) noting that $q_\infty = (1/2)\rho V^2$, we solve for $\dot{\gamma}$ and substitute for $\ddot{z}_1$ from equation (2)

$$\dot{\gamma} = \frac{\ddot{z}_1 - \dot{V}\gamma}{V} = \frac{C_{N_\alpha} \alpha \rho VA}{2m_1} + \frac{ky + b\dot{y}}{Vm_1} + \frac{C_x \rho VA}{2(m_1 + m_2)} \gamma \tag{12}$$

Differentiating equation (12), we get

$$\ddot{\gamma} = \frac{C_{N_\alpha} \dot{\alpha} \rho VA}{2m_1} + \frac{C_{N_\alpha} \alpha \dot{\rho} VA}{2m_1} + \frac{C_{N_\alpha} \alpha \rho \dot{V} A}{2m_1} + \frac{k\dot{y} + b\ddot{y}}{Vm_1}$$

$$- \frac{ky + b\dot{y}}{V^2} \dot{V} + \frac{C_x \rho \dot{V} A}{2(m_1 + m_2)} \gamma + \frac{C_x \dot{\rho} VA}{2(m_1 + m_2)} \gamma + \frac{C_x \rho VA}{2(m_1 + m_2)} \dot{\gamma} \tag{13}$$

If we substitute for $\dot{V}$ from equation (9) and $\dot{\gamma}$ from equation (12) and neglect second-order terms with products of coefficients such as $C_{N_\alpha} C_x$,

$$\ddot{\gamma} = \frac{C_{N_\alpha}\rho VA}{2m_1}\dot{\alpha} + \frac{C_{N_\alpha}\alpha\dot{\rho}VA}{2m_1} + \frac{C_x\dot{\rho}VA}{2(m_1 + m_2)}\gamma + \frac{k\dot{y} + b\ddot{y}}{Vm_1} \tag{14}$$

If the terms that are small relative to the other terms in equations (12) and (14) are eliminated

$$\dot{\gamma} = \frac{C_{N_\alpha}\alpha\rho VA}{2m_1} = \frac{C_{N_\alpha}\alpha q_\infty A}{Vm_1}$$

$$\ddot{\gamma} = \frac{C_{N_\alpha}\rho VA\dot{\alpha}}{2m_1} = \frac{C_{N_\alpha}q_\infty A\dot{\alpha}}{Vm_1}$$

If we now substitute for $\dot{\gamma}$ and $\ddot{\gamma}$ into equations (6) and (7) and then substitute for $\dot{\theta}$ and $\ddot{\theta}$ in equations (1) and (4),

$$I\ddot{\alpha} - \left[-\frac{C_{N_\alpha}q_\infty AI}{Vm_1} + q_\infty Ad\left(\frac{d}{V}\right)\left(C_{m_q} + C_{m_{\dot{\alpha}}}\right)\right]\dot{\alpha}$$

$$- C_{m_\alpha}\alpha q_\infty Ad - (ky + b\dot{y})x_b + \frac{m_2}{m_1 + m_2}F_x y = 0 \tag{15}$$

$$\ddot{z}_2 = \ddot{z}_1 + x_b\left(\ddot{\alpha} + \frac{C_{N_\alpha}\dot{\alpha}q_\infty A}{Vm_1}\right) + \ddot{y} \tag{16}$$

Note that the $(C_{m_q} + C_{m_{\dot{\alpha}}})\dot{\alpha}$ term in equation (15) is damping due to pitching and the $C_{N_\alpha}\dot{\alpha}$ terms in both equations (15) and (16) are damping terms due to plunging or swerving of the vehicle. Now equations (2), (3), (15), and (16) can be used to produce two simultaneous differential equations in α and y. Substituting into equation (16) for $\ddot{z}_1$ and $\ddot{z}_2$ from equations (2) and (3), we get

$$\ddot{y} + \left(\frac{m_1 + m_2}{m_1}\right)\left(\frac{b}{m_2}\right)\dot{y} + \left(\frac{m_1 + m_2}{m_1}\right)\left(\frac{k}{m_2}\right)y + x_b\ddot{\alpha} + \frac{F_N}{m_1} + x_b\frac{C_{N_\alpha}\dot{\alpha}q_\infty A}{Vm_1} = 0 \tag{17}$$

If we substitute for $(ky + b\dot{y})$ from equation (17) into equation (15),

$$\left(I + \frac{m_1m_2}{m_1 + m_2}x_b{}^2\right)\ddot{\alpha} - \left[-C_{N_\alpha}\frac{q_\infty A}{Vm_1}\left(I + \frac{m_1m_2}{m_1 + m_2}x_b{}^2\right) + q_\infty Ad\left(\frac{d}{V}\right)\left(C_{m_q} + C_{m_{\dot{\alpha}}}\right)\right]\dot{\alpha}$$

$$- C_{m_\alpha}\alpha q_\infty Ad + \frac{m_1m_2}{m_1 + m_2}x_b\ddot{y} + \frac{m_2}{m_1 + m_2}x_bF_N + \frac{m_2}{m_1 + m_2}F_x y = 0 \tag{18}$$

Rewriting equations (17) and (18) and substituting coefficients for F_N and F_x and abbreviating the $\dot{\alpha}$ coefficient in equation (18) with CMQ, we get

$$\ddot{y} + \left(\frac{m_1 + m_2}{m_1}\right)\left(\frac{b}{m_2}\right)\dot{y} + \left(\frac{m_1 + m_2}{m_1}\right)\left(\frac{k}{m_2}\right) y + x_b\ddot{\alpha} + \frac{q_\infty A}{m_1} C_{N_\alpha}\left(\alpha + \frac{\dot{\alpha}}{V} x_b\right) = 0 \tag{19}$$

$$\left(I + \frac{m_1 m_2}{m_1 + m_2} x_b^2\right)\ddot{\alpha} - \left[q_\infty Ad\left(\frac{d}{V}\right)(CMQ)\right]\dot{\alpha} - q_\infty Ad\left(C_{m_\alpha} - \frac{m_2}{m_1 + m_2} C_{N_\alpha} \frac{x_b}{d}\right)\alpha + \frac{m_1 m_2}{m_1 + m_2} x_b\ddot{y} + \frac{m_2}{m_1 + m_2} C_x q_\infty A y = 0 \tag{20}$$

Note that in equation (20) $\{I + [m_1m_2/(m_1 + m_2)]x_b^2\}$ is the moment of inertia about the instantaneous center of gravity of the system, designated I_{sys}, and that $\{C_{m_\alpha} - [m_2/(m_1 + m_2)]C_{N_\alpha}(x_b/d)\}$ is the pitching-moment curve slope for the system if the ballast is rigidly mounted, that is, $C_{m_{\alpha_{sys}}}$.

In equation (19) b can be expressed conveniently in terms of some fraction of critical damping. Critical damping will be arbitrarily defined here as that minimum value of b that would cause the ballast to lose its oscillatory behavior if it were mounted on a stationary platform. (This is not to be construed as the critical damping for the entire system; that quantity is undefined.) From simple harmonic-motion theory, then, $b_{crit} = 2\sqrt{km_2}$ and

$$b = \frac{b}{b_{crit}}\left(2\sqrt{km_2}\right) = \eta_R\left(2\sqrt{km_2}\right)$$

If $2\eta_R\sqrt{km_2}$ is substituted for b in equation (19), then

$$\ddot{y} + 2\frac{m_1 + m_2}{m_1}\eta_R\sqrt{\frac{k}{m_2}}\,\dot{y} + \frac{m_1 + m_2}{m_1}\left(\frac{k}{m_2}\right) y + x_b\ddot{\alpha} + \frac{q_\infty A}{m_1} C_{N_\alpha}\left(\alpha + \frac{\dot{\alpha}}{V} x_b\right) = 0 \tag{21}$$

Equations (20) and (21) must be solved numerically. However, some simplifying assumptions will enable the equations to be solved in closed form, and the solutions can be useful in indicating trends.

Closed-Form Solution

If q_∞ is assumed constant and the aerodynamic and spring damping (CMQ = η_R = 0) are neglected, equations (20) and (21) can be rewritten in the form

$$\ddot{\alpha} + K_1\alpha + K_2\ddot{y} + K_3 y = 0 \tag{22}$$

$$\ddot{y} + K_4\alpha + K_5\ddot{\alpha} + K_6 y = 0 \tag{23}$$

where

$$K_1 = \frac{-q_\infty Ad\left(C_{m_\alpha} - \frac{m_2}{m_1 + m_2} C_{N_\alpha} \frac{x_b}{d}\right)}{I + \frac{m_1 m_2}{m_1 + m_2} x_b^2}$$

$$K_2 = \frac{\frac{m_1 m_2}{m_1 + m_2} x_b}{I + \frac{m_1 m_2}{m_1 + m_2} x_b^2}$$

$$K_3 = \frac{\frac{m_2}{m_1 + m_2} C_x q_\infty A}{I + \frac{m_1 m_2}{m_1 + m_2} x_b^2}$$

$$K_4 = \frac{C_{N_\alpha} q_\infty A}{m_1}$$

$$K_5 = x_b$$

$$K_6 = \frac{m_1 + m_2}{m_1} \frac{k}{m_2}$$

Closed-form solutions can be written for these equations, and with initial conditions at $t = 0$, $\alpha = \alpha_o$, $y = y_o$, $\dot{\alpha} = \dot{\alpha}_o$, $\dot{y} = \dot{y}_o$ they can be expressed as

$$\left.\begin{aligned} y &= C_1 \cos \omega_1 t + C_2 \sin \omega_1 t + C_3 \cos \omega_2 t + C_4 \sin \omega_2 t \\ \alpha &= C_5 \cos \omega_1 t + C_6 \sin \omega_1 t + C_7 \cos \omega_2 t + C_8 \sin \omega_2 t \end{aligned}\right\} \quad (24)$$

(these expressions are valid only up to and including the point where frequency coalescence occurs, that is, $\omega_1 = \omega_2$) where

$$C_1 = \frac{Gy_o - \alpha_o}{G - H}$$

$$C_2 = \frac{G\,\frac{\dot{y}_o}{\omega_1} - \frac{\dot{\alpha}_o}{\omega_1}}{G - H}$$

$$C_3 = y_o - C_1$$

$$C_4 = \frac{\dot{y}_o - C_2\omega_1}{\omega_2}$$

$$C_5 = C_1 H$$

$$C_6 = C_2 H$$

$$C_7 = C_3 G$$

$$C_8 = C_4 G$$

and

$$G = \frac{(K_2 + 1)\omega_2{}^2 - (K_3 + K_6)}{(K_1 + K_4) - (K_5 + 1)\omega_2{}^2}$$

$$H = \frac{(K_2 + 1)\omega_1{}^2 - (K_3 + K_6)}{(K_1 + K_4) - (K_5 + 1)\omega_1{}^2}$$

From equation (24) we can express the primary natural frequencies of the cone and ballast, respectively,

$$\omega_1, \omega_2 = \left[\frac{A_1 \mp (A_1{}^2 - A_2)^{1/2}}{2}\right]^{1/2} \tag{25}$$

where

$$A_1 = \frac{K_3K_5 + K_2K_4 - K_6 - K_1}{K_2K_5 - 1}$$

$$A_2 = 4\left(\frac{K_3K_4 - K_1K_6}{K_2K_5 - 1}\right)$$

and K is defined as before. Frequency coalescence is defined as the condition where $\omega_1 = \omega_2$.

When frequency coalescence takes place, $(q_\infty/k)_{fc}$ can be written in terms of the body and aerodynamic-force parameters. From equation (25) it is apparent that frequency coalescence occurs ($\omega_1 = \omega_2$) when $A_1^2 - A_2 = 0$. If we substitute the above expressions for A_1 and A_2 into $A_1^2 - A_2 = 0$ and solve explicitly for $(q_\infty/k)_{fc}$

$$B_1 \left(\frac{q_\infty}{k}\right)_{fc}^2 + B_2 \left(\frac{q_\infty}{k}\right)_{fc} + B_3 = 0 \tag{26}$$

and

$$\left(\frac{q_\infty}{k}\right)_{fc} = \frac{-B_2 \pm (B_2^2 - 4B_1B_3)^{1/2}}{2B_1} \tag{27}$$

where

$$B_1 = \frac{m_2^2 A^2 x_b^2 C_x^2}{(m_1 + m_2)^2} + C_{m_\alpha}^2 A^2 d^2 + \frac{2m_2 A^2 d x_b^2 C_x C_{m_\alpha}}{m_1 + m_2} + \frac{4m_2 A^2 C_x C_{N_\alpha} I}{(m_1 + m_2)m_1}$$

$$B_2 = 2A\left[C_x\left(\frac{-x_b I}{m_1} - \frac{x_b^3 m_2}{m_1 + m_2}\right) + C_{N_\alpha}\left(\frac{-2x_b I}{m_1}\right) + C_{m_\alpha} d\left(\frac{m_1 + m_2}{m_1 m_2} I - x_b\right)\right]$$

$$B_3 = \left[\frac{I(m_1 + m_2)}{m_1 m_2} + x_b^2\right]^2$$

DISCUSSION OF RESULTS

A complete study of all the parameters that affect the oscillatory motion of the vehicle was not attempted. Rather, a specific cone with a given flight trajectory, in terms of time, velocity, and dynamic-pressure variation with altitude, was used as a model. The effects of spring stiffness and spring damping in the simulated ballast system and the effects of aerodynamic damping were investigated to ascertain their influence on the oscillatory frequency and amplitude of both the ballast and the vehicle. The influence of varying the ballast location is also examined briefly. The values used for the geometric parameters and aerodynamic coefficients are listed below (see sketch (a) or (b)):

$$d = 2.5 \text{ ft}$$

$$l = 7.0 \text{ ft}$$

$$x_{cg_{sys}} = 3.956 \text{ ft}$$

$x_{cg_{cone}}$ = 4.780 ft

x_{cp} = 4.928 ft

x_b = 2.36 ft

m_1 = 12.36 slugs

m_2 = 6.64 slugs

I = 44.44 slug-ft^2 (I_{sys} = 68.5)

C_{N_α} = 1.95

C_x = 0.075

C_{m_α} = -0.110 ($C_{m_{\alpha_{sys}}}$ = -0.753)

$C_{m_q} + C_{m_{\dot{\alpha}}}$ = 0, -1.5

The flight trajectory used for the investigation is shown in figure 1, where velocity, dynamic pressure, and oscillatory frequency for a rigid system (infinite spring constant) are shown for an altitude range from 200,000 to 20,000 feet. Also shown is elapsed time with t = 0.0 at h = 200,000 feet. The initial entry angle was taken to be -22°.

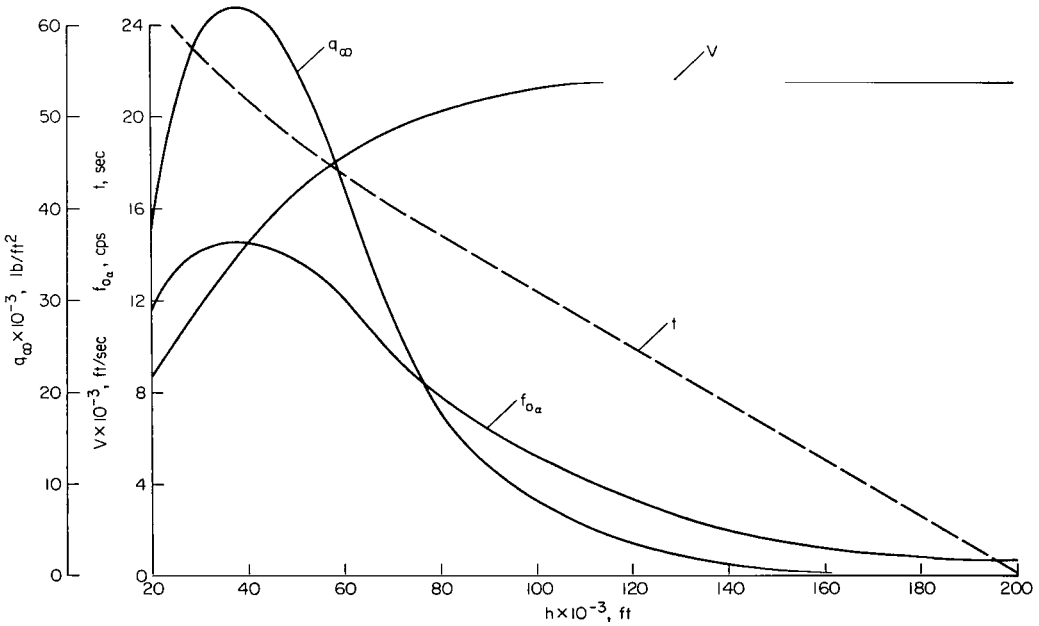

Figure 1.- Flight trajectory parameters for example case.

Oscillatory motions of both conical vehicle and ballast were obtained by integrating numerically the coupled equations (20) and (21), where V and q_∞ were entered in tabular form as functions of time. The motions were started at the velocity and dynamic pressure corresponding to 200,000 feet altitude. The other initial conditions were $\alpha = 0.2$ rad, $\dot{\alpha} = 0$, $y = 0$, $\dot{y} = 0$. The resulting motions were then studied to determine the frequency and amplitude behavior of both cone and ballast and to determine whether conditions might occur at which the cone angle-of-attack oscillations would be divergent.

Figure 2 shows typical motions of cone and ballast as functions of time. For this case $k = 5{,}000$ lb/ft, $n_R = 0$, and $C_{m_q} + C_{m_{\dot{\alpha}}} = 0$. Initially the primary oscillatory frequencies of the two motions are much different. At high altitude (where q_∞ is very small), the ballast oscillates at a primary frequency, f_y, near the natural frequency for a two-body system uninfluenced by any external forces or moment; that is,

$$f_y = \frac{1}{2\pi}\sqrt{\frac{k}{m_2}}\left(\frac{m_1 + m_2}{m_1} + \frac{m_2 x_b^2}{I}\right)^{1/2} = \left(\frac{m_1 + m_2}{m_1} + \frac{m_2 x_b^2}{I}\right)^{1/2} f_{o_y} \tag{28}$$

where f_{o_y} is the natural frequency of a simple mass spring-mounted to a rigid platform. The frequency is about 6.7 cps, nearly equal to the 6.73 cps calculated from equation (28) estimated for flight in a vacuum (where $q_\infty = 0$). (The ballast frequency, f_{o_y}, would be 4.37 cps if the cone were held stationary.) Initially each motion for y and α has a secondary natural frequency, which is simply the other's primary natural frequency. As the dynamic pressure increases with time, the primary oscillatory frequency, f_α, of the cone increases at a faster rate than would be expected for a rigid system. The difference is shown in figure 3, where f_α is plotted as measured directly from the motion in figure 2 and f_{o_α} is the frequency for a rigid system. Since only a portion of the ballast motion in figure 2 exhibits a primary frequency that can be measured directly, the f_y curve was calculated from the closed-form solution (eq. (25)) for various values of q_∞ and then plotted versus the corresponding time, t. The closed-form solution agreed perfectly with f_α and f_y that were measurable from figure 2. It is evident that as q_∞ increases (and consequently f_α), the primary ballast frequency decreases until at $t = 10.2$ seconds the ballast and cone frequencies are the same (frequency coalescence). However, figure 2 shows that the motion diverges at $t \sim 9.2$ seconds, that is, before frequency coalescence takes place. Despite the onset of divergence the frequencies behave as predicted by equation (25). The amplitude of both cone and ballast increase until the ballast motion is bounded by the cone walls. At this point ($t = 10.3$ sec, see fig. 2) describing the motion of the system becomes more complex and is beyond the scope of this investigation.

Some motions obtained from closed-form solutions help to understand why the coupled motion of the ballast and cone cause divergence prior to frequency coalescence. Figure 4 illustrates ballast and cone motions at constant values of q_∞ corresponding to values just prior to and at frequency coalescence.

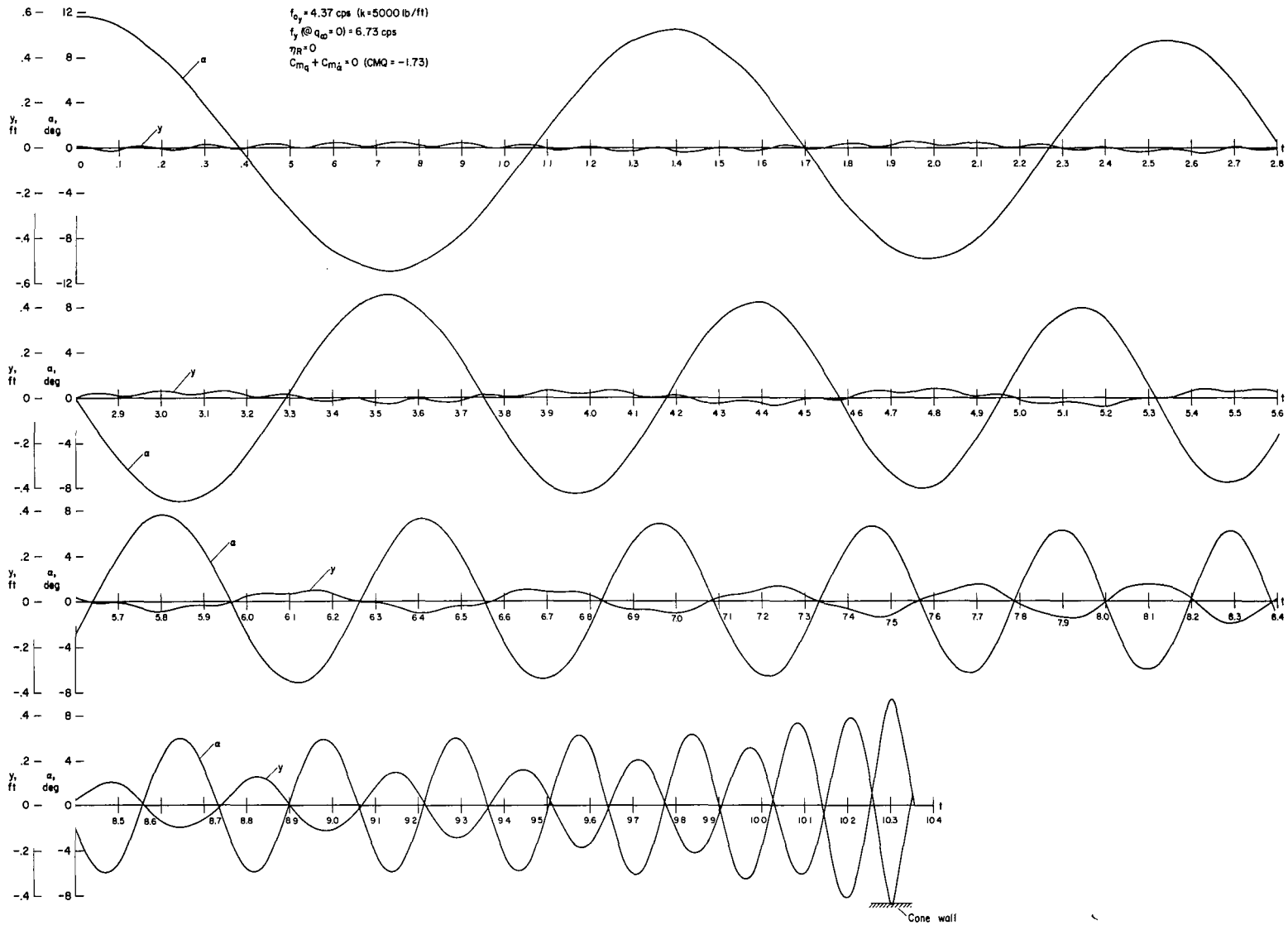

Figure 2.- Typical cone and ballast motion for example case.

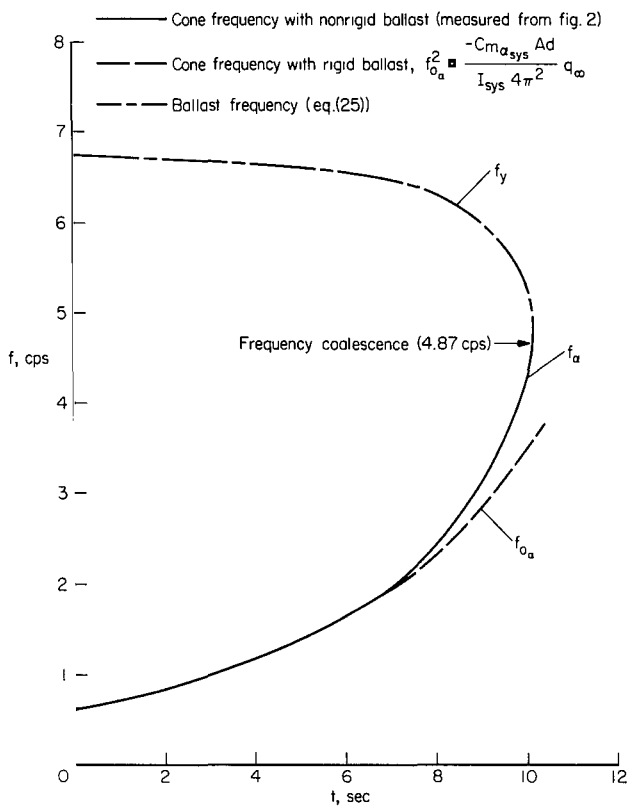

Figure 3.- Comparison of frequencies for rigid and nonrigid systems.

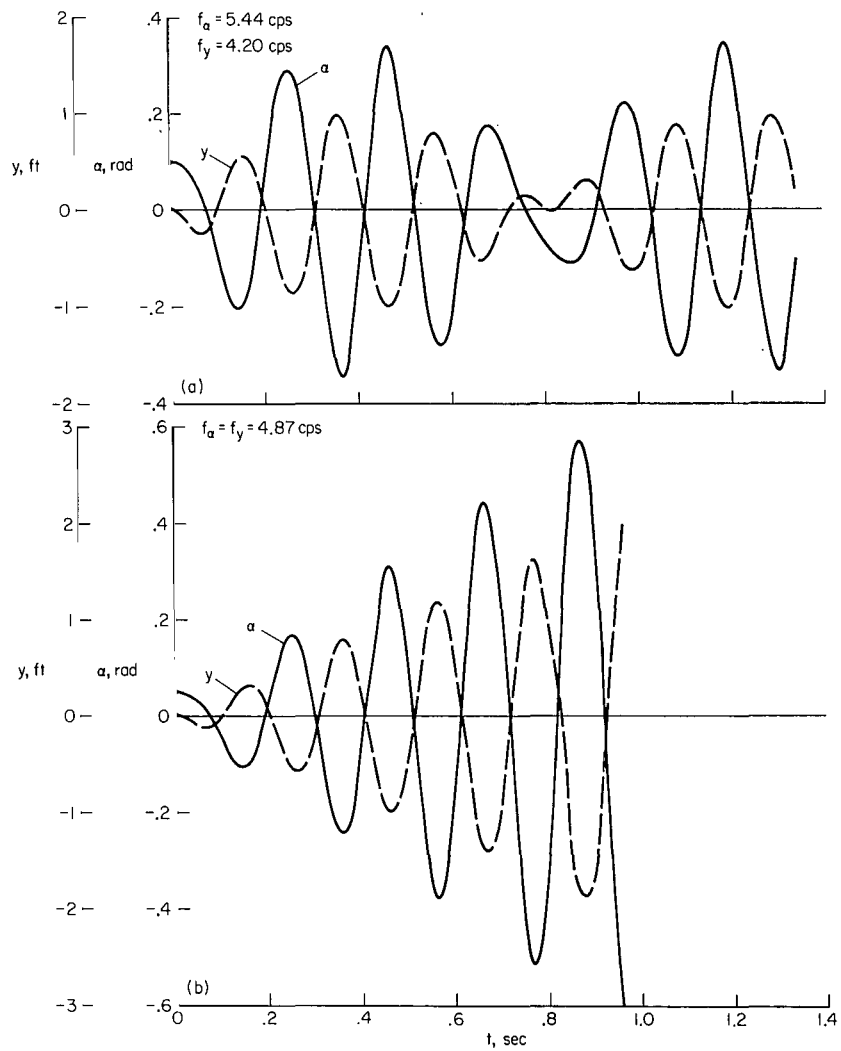

(a) q_∞ = 3500 lb/ft^2.
(b) q_∞ = 3774 lb/ft^2 (frequency coalescence).

Figure 4.- Oscillatory motion of cone and ballast at constant dynamic pressure.

When the two bodies oscillate at nearly identical natural frequencies (fig. 4(a)), a "beat frequency" is established in which the ballast motion first lags, then leads the cone motion. At frequency coalescence (fig. 4(b)) the ballast lags continuously. Applying this quasi-steady interpretation of the lag phenomenon to the variable q_∞ case in figure 2, we conclude that the divergent motion occurs somewhat before frequency coalescence is reached because of the >180° lag of the ballast that is typical of part of the beat frequency motion. Because q_∞ is continuously increasing, the beat frequency does not fully form and the ballast lags continuously until coalescence.

The effect of the ballast on the cone motion is illustrated in figure 5 where the amplitude history of the cone with a nonrigid ballast is compared to one calculated for a completely rigid system. Note that for the rigid body the amplitude decreases despite the fact that $C_{m_q} + C_{m_{\dot{\alpha}}} = 0$ because of the increasing q_∞ with time and the damping contribution from plunging. It is apparent that the amplitude ratio is affected by the ballast long before frequency coalescence conditions occur; in fact, the motion diverges before coalescence conditions are reached because of the >180° lag discussed above. The point at which the ballast reaches the cone wall is also indicated.

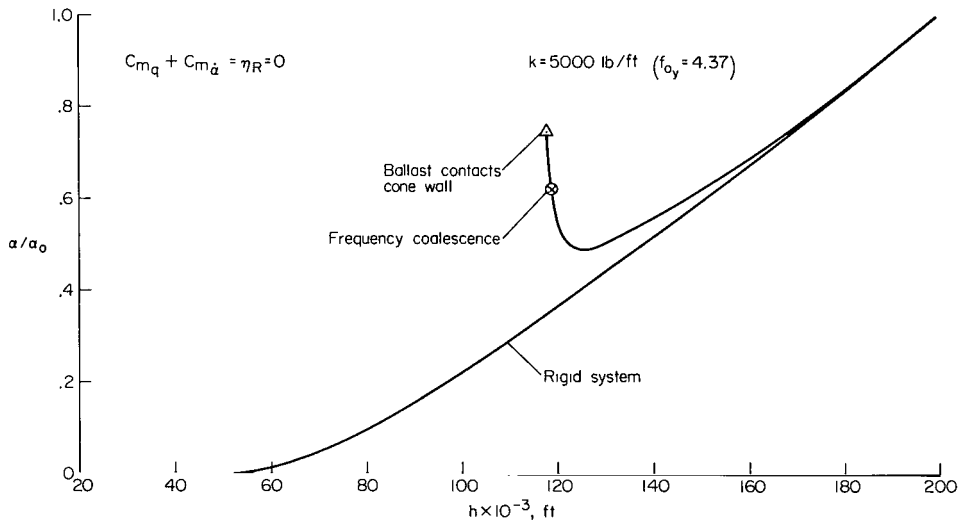

Figure 5.- Envelope of oscillatory cone motion.

Effects of Changing Spring Force and Damping Constants

To see what effect a change in spring stiffness or the addition of damping to the ballast system has on the cone oscillatory history, amplitude ratio (where α_o is 0.2 rad at h = 200,000 ft) versus altitude is plotted in

figure 6 for three different spring constants k = 5,000, 15,000, and 50,000 lb/ft. For comparison, the amplitude ratio for a rigid system is also shown. The damping-in-pitch parameter, $C_{m_q} + C_{m_{\dot{\alpha}}}$, and ballast damping, η_R, are both zero. The effect of decreasing the stiffness (decreasing k) of the ballast is to produce oscillatory divergence at a higher altitude (and lower q_∞).

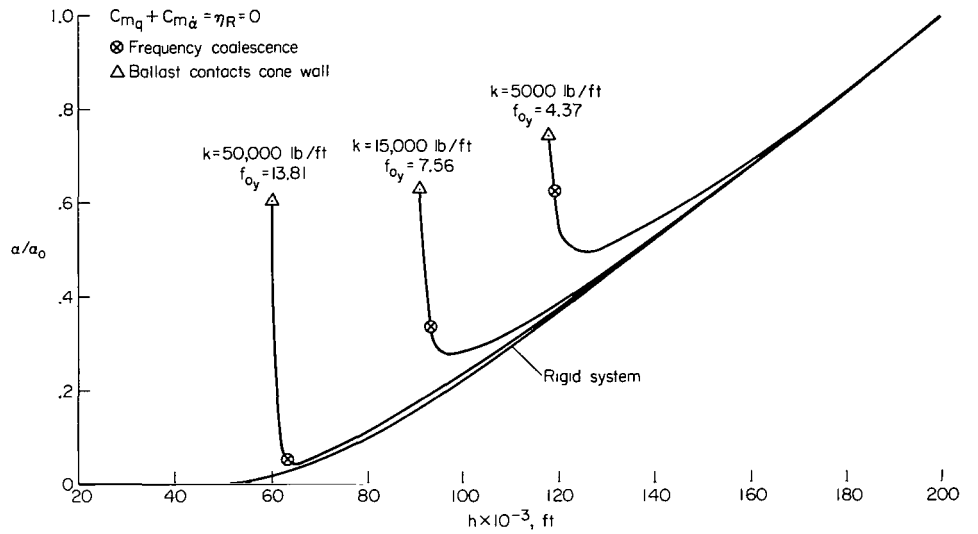

Figure 6.- Envelope of oscillatory cone motion for three different spring stiffnesses.

Ballast damping.- Figure 7 shows the effect of introducing damping into the ballast system for three different spring constants. The damping values go to a practical upper limit of $\eta_R = 1.0$ (the critical damping value for the ballast system if the ballast were attached to a rigid platform) and the effect of increased damping is to cause divergence to occur sooner in the flight. The reason is simply that if the ballast system includes damping, the ballast will lag behind the cone sooner than it would if there were no internal damping. In all cases the amplitude ratio is plotted until the ballast contacts the cone wall or the amplitude ratio increases to 1.0, whichever occurs first.

Aerodynamic damping.- Figure 8 shows that aerodynamic damping delays the onset of divergence, as one would expect. Note also that for the rigid-body case there is no divergence during the decreasing dynamic pressure part of the trajectory (i.e., altitudes below 37,000 ft), in either case because even when $C_{m_q} + C_{m_{\dot{\alpha}}} = 0$, there is sufficient damping from the plunging motion ($C_{N_\alpha}\dot{\alpha}$ term) to prevent divergence in angle of attack.

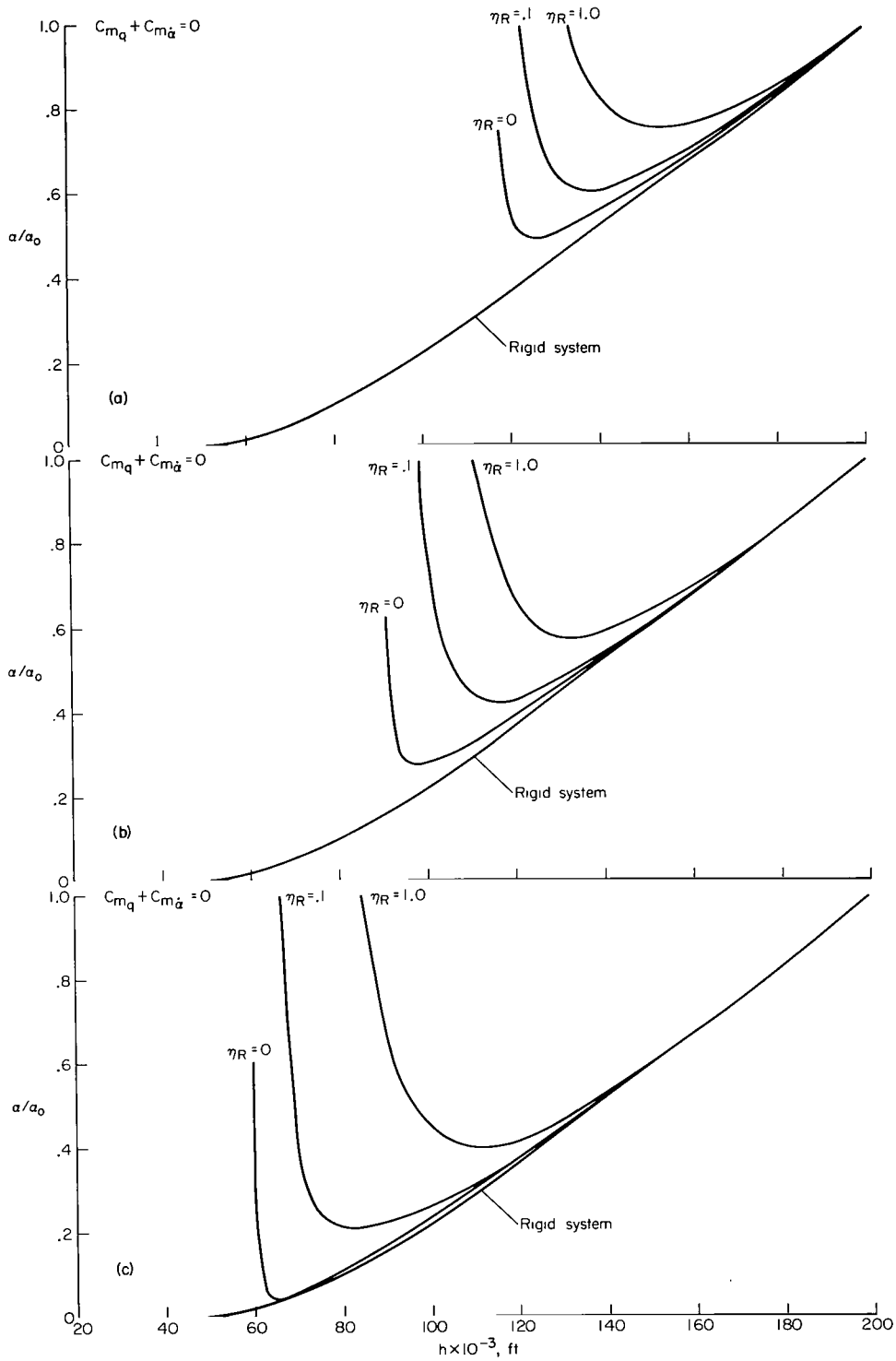

(a) k = 5,000 lb/ft (f_{o_y} = 4.37 cps).

(b) k = 15,000 lb/ft (f_{o_y} = 7.56 cps).

(c) k = 50,000 lb/ft (f_{o_y} = 13.81 cps).

Figure 7.- Envelope of oscillatory cone motion for various ballast damping conditions.

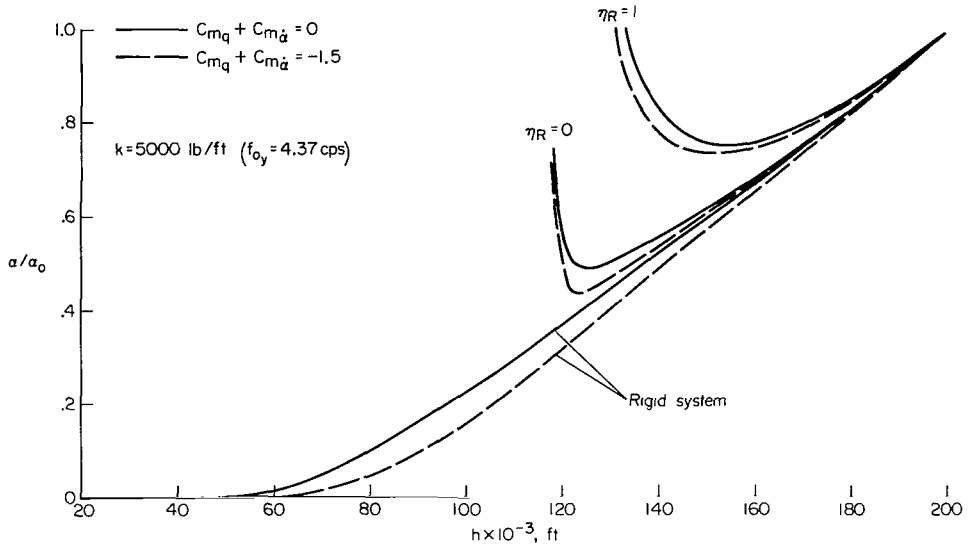

Figure 8.- Effect of aerodynamic damping on cone amplitude history.

Results From Closed-Form Solutions

We have already seen in the discussion of figure 3 that the closed-form solutions are very useful for calculating frequency histories (eq. (25)) by using discrete points along the trajectory and for calculating the point in the trajectory where a frequency coalescence condition exists ($q_{\infty_{fc}}$ can be calculated directly from eq. (27) and this in turn can be related to a specific time, t, from fig. 1).

In addition the closed-form solution (eq. (27)) can be used to determine the effect of the longitudinal location of the ballast on the coalescence point for the system. In figure 9 $(q_\infty/k)_{fc}$ is plotted as a function of the

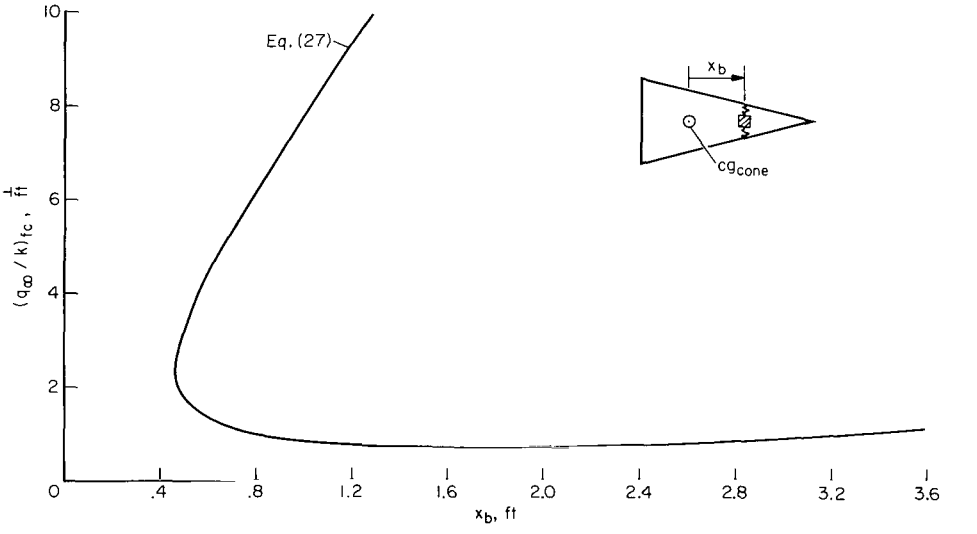

Figure 9.- Variation of dynamic pressure to spring stiffness ratio at frequency coalescence with ballast location.

ballast location x_b. The most important point is that if the ballast location is less than $x_b = 0.465$ ft, there is no theoretical frequency coalescence. Above $x_b = 0.465$ there are two q_∞/k conditions that will produce coalescence although the lower one is more significant since it would be the first to be encountered in an atmosphere entry. This coalescence point can, of course, be coordinated with a specific altitude by using the q_∞ history with altitude (as in fig. 1). It should be emphasized that this criterion for minimum x_b to produce frequency coalescence is for the specific body parameters used in this paper and would be numerically different if the body dimensions or aerodynamic coefficients in equation (27) were changed.

CONCLUSIONS

The effects of a nonrigidly supported ballast on the dynamic behavior of a slender body with linear aerodynamics descending through the atmosphere in planar motion have been investigated. Some important conclusions can be drawn.

The point at which frequency coalescence (ballast and cone frequencies are equal) occurs in a flight with variable dynamic pressure can be predicted accurately by means of closed-form solutions if constant values of dynamic pressure are assumed and aerodynamic and ballast damping are ignored. However, it has been shown that the amplitude of oscillations diverges before frequency coalescence is experienced. This amplitude divergence is caused by the continuous >180° phase lag of the ballast motion relative to that of the cone just prior to frequency coalescence. (Phase lag is exactly 180° at frequency coalescence.) In addition, it was found that

1. Decreasing the stiffness of the ballast support causes divergence earlier in the flight (higher altitude and lower dynamic pressure).

2. Introducing damping into the ballast system (at least up to the point of critical damping for the ballast mounted on a stationary platform) produces the phase lag sooner in the flight than if there were no internal damping and therefore promotes earlier divergence of the oscillations.

3. Aerodynamic damping delays the onset of divergence.

4. Varying the ballast longitudinal location has large effects on the altitude at which divergence occurs. There is a minimum distance from the cone center of gravity to the ballast location below which no frequency coalescence can exist.

Ames Research Center
National Aeronautics and Space Administration
Moffett Field, Calif., 94035, Sept. 29, 1969

NATIONAL AERONAUTICS AND SPACE ADMINISTRATION
WASHINGTON, D. C. 20546

OFFICIAL BUSINESS

FIRST CLASS MAIL

POSTAGE AND FEES PAID
NATIONAL AERONAUTICS AND
SPACE ADMINISTRATION

"The aeronautical and space activities of the United States shall be conducted so as to contribute . . . to the expansion of human knowledge of phenomena in the atmosphere and space. The Administration shall provide for the widest practicable and appropriate dissemination of information concerning its activities and the results thereof."

—NATIONAL AERONAUTICS AND SPACE ACT OF 1958

NASA SCIENTIFIC AND TECHNICAL PUBLICATIONS

TECHNICAL REPORTS: Scientific and technical information considered important, complete, and a lasting contribution to existing knowledge.

TECHNICAL NOTES: Information less broad in scope but nevertheless of importance as a contribution to existing knowledge.

TECHNICAL MEMORANDUMS: Information receiving limited distribution because of preliminary data, security classification, or other reasons.

CONTRACTOR REPORTS: Scientific and technical information generated under a NASA contract or grant and considered an important contribution to existing knowledge.

TECHNICAL TRANSLATIONS: Information published in a foreign language considered to merit NASA distribution in English.

SPECIAL PUBLICATIONS: Information derived from or of value to NASA activities. Publications include conference proceedings, monographs, data compilations, handbooks, sourcebooks, and special bibliographies.

TECHNOLOGY UTILIZATION PUBLICATIONS: Information on technology used by NASA that may be of particular interest in commercial and other non-aerospace applications. Publications include Tech Briefs, Technology Utilization Reports and Notes, and Technology Surveys.

Details on the availability of these publications may be obtained from:

SCIENTIFIC AND TECHNICAL INFORMATION DIVISION

NATIONAL AERONAUTICS AND SPACE ADMINISTRATION

Washington, D.C. 20546